

Transition wavelengths and probabilities for spectral lines of Zr III

M.C. Martins^{1,3,a}, J.P. Santos^{2,3}, A.M. Costa^{1,3}, and F. Parente^{2,3}

¹ Departamento Física, Faculdade de Ciências, Universidade de Lisboa, Campo Grande, 1749-016 Lisboa, Portugal

² Departamento de Física, Faculdade de Ciências e Tecnologia, Universidade Nova de Lisboa, Monte de Caparica, 2825-114 Caparica, Portugal

³ Centro de Física Atómica da Universidade de Lisboa, Av. Prof. Gama Pinto 2, 1649-003 Lisboa, Portugal

Received 27 December 2005 / Received in final form 7 March 2006

Published online 5 May 2006 – © EDP Sciences, Società Italiana di Fisica, Springer-Verlag 2006

Abstract. Wavelengths and oscillator strengths for all $4d4f \rightarrow 4d^2$ dipole-allowed fine-structure transitions in Zr III have been calculated within the Multi-Configuration Dirac-Fock method with QED corrections. These transitions are included in the spectrum of some chemically peculiar stars, like the B-type star χ Lupi observed by the Hubble space telescope. The results are compared to existing experimental and semi-empirical data.

PACS. 31.25.Jf Electron correlation calculations for atoms and ions: excited states – 32.30.Jc Visible and ultraviolet spectra – 32.70.Cs Oscillator strengths, lifetimes, transition moments

1 Introduction

Chemically peculiar stars are identified by the presence of anomalously strong (or weak) absorption lines of certain elements in their spectra. These stars are known to have a large number of spectral lines, many of which from elements with low solar abundance [1]. The observed overabundances of these elements have been under scrutiny over the years and different explanations have been proposed [2]. The determination of the abundance of a species requires both accurate wavelengths and oscillator strengths for inclusion in the spectrum synthesis.

The first studies of these spectra were based on the International Ultraviolet Explorer (IUE) satellite observations. The IUE was launched in 1978 and operated over the 1200–3200 Å region of the near and far ultraviolet.

More recently, in a investigation of the χ Lupi star spectra, obtained with the Goddard high-resolution spectrograph on the Hubble Space Telescope, Leckrone et al. [3] have identified a number of absorption lines in the ultra-violet region as belonging to the Zr III ion.

The most recent analysis of the spectrum of Zr III, reported by Reader and Acquista in 1997 [4], provided for the first time accurate wavelength values. The analyzed spectrum was obtained with a sliding spark discharge at the National Institute of Standards and Technology (NIST).

Although it is fairly straightforward to obtain line wavelengths in this region of the spectrum [5], it is far

more difficult to do accurate measurements of transition probabilities.

Charro, López-Ayuso and Martín published in 1999 [6] calculated values of oscillator strengths in the LSJ -coupling scheme using the semi-empirical quantum-defect orbital method for some of the dipole-allowed fine-structure transitions in Zr III between the levels belonging to $4d^2$ and $4dnl$ ($n = 4-6$ and $\ell = 1-3$) configurations. This method depends on some parameters, namely the quantum defects, that are extracted from experimental data. On the other hand, Reader and Acquista calculated weighted oscillator strengths using the wave functions obtained with the fitted values of the energy parameters [4].

A detailed comparison between the two sets of oscillator strength values show that many lines reported by Reader and Acquista were not accounted for in Charro et al. work. Furthermore, many discrepancies can be found between the two sets of data.

In the present *ab initio* theoretical work we start from a Dirac-Fock calculation with Breit interaction included self-consistently. Both correlation and relativistic effects are taken into account as they play a significant role in the energy and transition probabilities calculations of this atomic species ($Z = 40$). Higher-order retardation and one-electron radiative corrections are also included, and the screening of the self-energy is evaluated using the Welton approximation. Correlation is added within the Multi-Configuration Dirac-Fock method (MCDF). In this framework we have calculated the relativistic transition wavelengths for all Zr III $4d4f \rightarrow 4d^2$ fine-structure lines,

^a e-mail: mdmartins@fc.ul.pt

and used them to compute the corresponding oscillator strengths.

2 Calculation of atomic wave functions, energies and transition probabilities

Bound state wave functions and radiative transition probabilities were calculated using the multi-configuration Dirac-Fock program of Desclaux and Indelicato [7,8]. The program was used in multi-configuration mode because correlation was found to be important for the transition energies and oscillator strengths. The wave functions of the initial and final states were computed independently, that is, atomic orbitals were fully relaxed in the calculation of the wave function for each state, and non-orthogonality was taken in account in transition probability calculations.

In order to obtain a correct relationship between many-body methods and quantum electrodynamics (QED) [9–12], one should start from the no-pair Hamiltonian

$$\mathcal{H}^{\text{no pair}} = \sum_{i=1}^N \mathcal{H}_D(r_i) + \sum_{i<j} \mathcal{V}(|\mathbf{r}_i - \mathbf{r}_j|), \quad (1)$$

where \mathcal{H}_D is the one electron Dirac operator and \mathcal{V} is an operator representing the electron-electron interaction of order one in α , properly set-up between projection operators $A_{ij}^{++} = A_i^+ A_j^+$ to avoid coupling positive and negative energy states

$$\mathcal{V}_{ij} = A_{ij}^{++} V_{ij} A_{ij}^{++}. \quad (2)$$

The expression of V_{ij} in the Coulomb gauge and in atomic units is

$$V_{ij} = \frac{1}{r_{ij}} \quad (3a)$$

$$- \frac{\boldsymbol{\alpha}_i \cdot \boldsymbol{\alpha}_j}{r_{ij}} \quad (3b)$$

$$- \frac{\boldsymbol{\alpha}_i \cdot \boldsymbol{\alpha}_j}{r_{ij}} \left[\cos\left(\frac{\omega_{ij} r_{ij}}{c}\right) - 1 \right] + c^2 (\boldsymbol{\alpha}_i \cdot \nabla_i) (\boldsymbol{\alpha}_j \cdot \nabla_j) \frac{\cos\left(\frac{\omega_{ij} r_{ij}}{c}\right) - 1}{\omega_{ij}^2 r_{ij}}, \quad (3c)$$

where $r_{ij} = |\mathbf{r}_i - \mathbf{r}_j|$ is the inter-electronic distance, ω_{ij} is the energy of the exchanged photon between the two electrons, $\boldsymbol{\alpha}_i$ are the Dirac matrices and c is the speed of light. We use the Coulomb gauge as it has been demonstrated that it provides energies free from spurious contributions at the ladder approximation level and must be used in many-body atomic structure calculations [13,14].

The term (3a) represents the Coulomb interaction, the term (3b) is the Gaunt (magnetic) interaction, and the last two terms (3c) stand for the retardation operator. In this expression the ∇ operators act only on r_{ij} and not on the following wave functions.

By a series expansion of the operators in expressions (3b) and (3c) in powers of $\omega_{ij} r_{ij}/c \ll 1$ one obtains

the Breit interaction, which includes the leading retardation contribution of order $1/c^2$. The Breit interaction is, then, the sum of the Gaunt interaction (3b) and the Breit retardation

$$B_{ij}^R = \frac{\boldsymbol{\alpha}_i \cdot \boldsymbol{\alpha}_j}{2r_{ij}} - \frac{(\boldsymbol{\alpha}_i \cdot \mathbf{r}_{ij})(\boldsymbol{\alpha}_j \cdot \mathbf{r}_{ij})}{2r_{ij}^3}. \quad (4)$$

In the many-body part of the calculation the electron-electron interaction is described by the sum of the Coulomb and the Breit interactions. Higher orders in $1/c$, deriving from the difference between equations (3c) and (4) are treated here only as a first order perturbation.

All calculations are done for finite nuclei using uniformly charged spheres.

Finally, from a full QED treatment, one also obtains the radiative corrections (important for the innermost shells) to the electron-nucleus interaction (self-energy and vacuum polarization) [15–22].

For each transition, initial and final states are computed independently to get accurate correlation energies. Consequently, the initial and final state orbitals of identical symmetry are not orthogonal (see, e.g. [23] and references therein). This non-orthogonality is properly taken in account in the transition probability calculation using Löwdin's method [24]. Being a fully relativistic method, initial and final levels for each transition are defined in jj -coupling. However, for comparison with other published work where levels are characterized by their LSJ values, we show in the tables, for each level, the most important LSJ set of values which results from the expansion of the jjJ wave function in terms of LSJ ones.

3 Discussion and results

Unlike the evaluation of energies, there is no guaranteed monotonic improvement in the values of oscillator strengths as the virtual orbital space spanned is expanded. Hibbert [25,26] suggested several indicators to assess the degree of accuracy which can be claimed for a calculation.

One of those indicators is the agreement with calculations by other authors and with experimental results. Since in the present case existing calculations are semi-empirical this indicator is inconclusive, and experimental results are not available.

Another requisite is the agreement between length and velocity forms of the oscillator strength. Although this is not a proof of accuracy, since it will be fulfilled for any local potential, it is nevertheless a desirable requisite. When there is no good agreement between the two forms, there are reasons for a preference of the length form over the velocity form from the non-relativistic [27,28] and relativistic [29] points of view.

The most effective indicator is provided by a study of the oscillator strengths evolution as the virtual orbital space is enlarged. This will enable us to see how dependent the results are on the included orbitals.

To obtain the valence and the core-valence correlation contributions we used a virtual space spanned by doubly-excited configurations up to the $6p$ orbitals resulting from

Table 1. Correlation effect on $[\text{Ar}] 3d^{10} 4s^2 4p^6 4d 4f \ ^1P_1 \rightarrow [\text{Ar}] 3d^{10} 4s^2 4p^6 4d^2 \ ^1S_0$ transition wavelength and oscillator strengths. The $[\text{Ar}] 3d^{10}$ core is omitted in the table entries.

Initial state (1P_1)	Final state (1S_0)	$\lambda(\text{\AA})$	f_{length}	f_{velocity}
$4s^2 4p^6 4d 4f$	$4s^2 4p^6 4d^2$	1132.1	0.543	0.569
	$+4s^2 4p^5 4d^2 4f$	1071.8	0.507	0.573
	$+4s^2 4p^6 4f^2$	1023.1	0.466	0.613
$+4s^2 4p^5 4d 4f^2 + 4s 4p^6 4f^3$		1025.3	0.483	0.657
$+4s^2 4p^5 4d (5s^2 + 5p^2)$	$+4s^2 4p^6 (5s^2 + 5p^2)$	996.2	0.493	0.607
$+4s^2 4p^6 5s 5p$		985.2		
$+4s^2 4p^5 4d (5d^2 + 5g^2 + 6s^2 + 6p^2)$	$+4s^2 4p^6 (5d^2 + 5g^2 + 6s^2 + 6p^2)$	983.4	0.522	0.572
$+4s^2 4p^5 4d 5f^2$	$+4s^2 4p^6 5f^2$	982.2	0.522	0.574
$+4s^2 4p^5 5s 5f^2$		982.2	0.521	0.572
$\lambda_{\text{exp}} [4]$		972.174		

Table 2. Correlation effect on $[\text{Ar}] 3d^{10} 4s^2 4p^6 4d 4f \ ^3D_3 \rightarrow [\text{Ar}] 3d^{10} 4s^2 4p^6 4d^2 \ ^3P_2$ transition wavelength and oscillator strengths. The $[\text{Ar}] 3d^{10}$ core is omitted in the table entries.

Initial state (3D_3)	Final state (3P_2)	$\lambda(\text{\AA})$	f_{length}	f_{velocity}
$4s^2 4p^6 4d 4f$	$4s^2 4p^6 4d^2$			
$+4s 4p^6 4d^2 4f$		929.8	0.299	0.279
$+4s^2 4p^5 4f^2 5s$	$+4s^2 4p^6 4f^2$	913.7	0.308	0.313
$+4s^2 4p^5 4d (5s^2 + 5p^2)$	$+4s^2 4p^4 4d^2 5s^2 + 4s^2 4p^6 5p^2$	910.7	0.305	0.307
	$+4s^2 4p^6 4d 5s$	910.4	0.285	0.288
$+4s^2 4p^5 4d 5d^2$	$+4s^2 4p^6 5d^2$	906.5	0.293	0.287
$+4s^2 4p^5 4d 5g^2$	$+4s^2 4p^6 (5f^2 + 5g^2)$	904.9	0.294	0.287
$+4s^2 4p^5 4d (6s^2 + 6p^2)$	$+4s^2 4p^4 4d^2 (6s^2 + 6p^2)$	904.7	0.294	0.286
$+4s^2 4p^5 5s 5f^2$		904.7	0.294	0.286
	$+4s^2 4p^6 4d 6s$	904.3	0.250	0.245
$\lambda_{\text{exp}} [4]$		868.612		

the excitation of $n = 4$ electrons in the initial and final states because we found that higher orbitals give no appreciable contribution to correlation. In this way, we were able to maintain a manageable virtual orbital space.

The virtual space included also some single-excited configurations limited to the $n = 4$ shell, such as the $4s^2 4p^5 4d 4f^2$ and the $4s 4p^6 4d^2 4f$ in the initial state and the $4s^2 4p^5 4d^2 4f$ and $4s 4p^6 4d^3$ in the final state. These configurations give a significant contribution to the transition energy and/or oscillator strength in some transitions, such as the one illustrated in Table 1.

Furthermore, we also considered some single-excited configurations suggested in Reader and Acquista's work [4], namely the $4s^2 4p^6 4d 5s$ and $4s^2 4p^6 4d 6s$ configurations in the final state. These configurations have a non-negligible influence in both the transition energy and the oscillator strength: the first one in the 1D_2 , 3P_2 and the 3F_3 levels, and the last one in the 3P_2 level. An example is shown in Table 2.

The results obtained in this work for the $4d 4f \ ^1P_1 \rightarrow 4d^2 \ ^1S_0$ transition wavelength, shown in Table 1, are an example of the importance of correlation on this quantity. We observe that the calculated single-configuration Dirac-Fock wavelength differs by about 16% from the experimental value. The inclusion of correlation narrows this difference to about 1%. Furthermore, we note that, for in-

stance, in the final state the LS percentage composition is 94.3% for the $4d^2 \ ^1S$ and 3.4% for the $5s^2 \ ^1S$, which is in agreement with the values of Reader and Acquista [4].

Another example concerns the $4d 4f \ ^1G_4 \rightarrow 4d^2 \ ^3F_3$ transition. Inclusion of the same type of correlation changed the calculated wavelength from $\lambda = 877.4 \text{ \AA}$, obtained with single-configuration wave functions, to $\lambda = 842.6 \text{ \AA}$. The latter differs only by about 0.5% from the experimental value $\lambda_{\text{exp}} = 838.259 \text{ \AA}$ measured by Reader and Acquista [4].

In Table 3, we provide the results obtained in this work for the wavelengths and oscillator strengths, calculated with the theoretical energies computed in this work, of all $4d 4f \rightarrow 4d^2$ dipole-allowed fine-structure transitions in Zr III. For comparison, the available experimental transition wavelengths [4] and existing semi-empirical oscillator strength values [6,4] are also included.

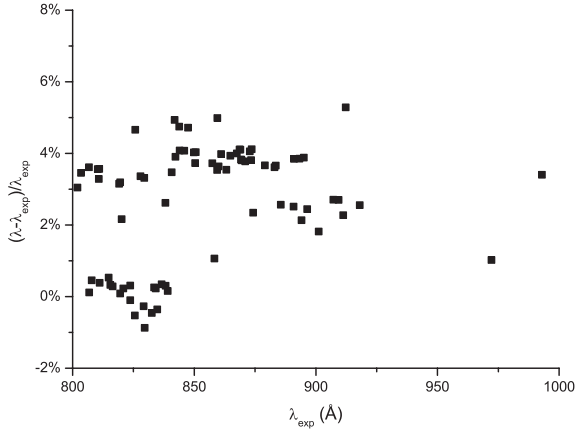
A comparison between the results of this work for the wavelengths and Reader and Acquista's experimental results [4] is presented in Figure 1. We observe that all theoretical results differ by less than 5% from the experimental ones, and one fourth of these theoretical results differ by less than 1% from the Reader and Acquista's results. This agreement certainly contributes for confirming the validity of Reader and Acquista's assignments.

Table 3. Theoretical wavelengths (λ) and oscillator strengths in the length (f_{length}) and velocity (f_{velocity}) gauges calculated in this work, and semi-empirical theoretical oscillator strengths (f_{set}) calculated by Charro et al. [6] and by Reader and Acquista [4]. The experimental wavelengths (λ_{exp}) are from Reader and Acquista [4]. The wavelengths are listed in Å units.

Initial	Final	λ	λ_{exp} [4]	f_{length}	f_{velocity}	f_{set} [6]	f_{set} [4]
1D_2	3P_1	911.3	879.034	1.48×10^{-2}	1.65×10^{-2}		2.41×10^{-2}
1D_2	3F_2	844.9	819.078	3.63×10^{-3}	3.75×10^{-3}		5.26×10^{-3}
1D_2	1D_2	902.4	859.516	1.83×10^{-1}	2.11×10^{-1}	2.30×10^{-1}	2.35×10^{-1}
1D_2	3P_2	914.9	883.015	8.04×10^{-4}	7.28×10^{-4}		
1D_2	3F_3	824.6	823.683	2.07×10^{-4}	1.69×10^{-4}		
1F_3	3F_2	839.9	810.966	1.85×10^{-2}	1.53×10^{-2}		1.66×10^{-2}
1F_3	1D_2	884.9	850.583	2.59×10^{-1}	2.45×10^{-1}	5.40×10^{-1}	3.17×10^{-1}
1F_3	3P_2	909.1	873.593	1.07×10^{-1}	1.12×10^{-1}		1.26×10^{-1}
1F_3	3F_3	819.9	815.474	1.20×10^{-2}	1.06×10^{-2}		1.01×10^{-2}
1F_3	3F_4	824.5	820.861	1.05×10^{-2}	1.23×10^{-2}		2.12×10^{-2}
1F_3	1G_4	915.3	890.796	1.48×10^{-3}	3.22×10^{-3}		1.06×10^{-2}
1G_4	3F_3	842.6	838.259	1.14×10^{-2}	1.03×10^{-2}		1.53×10^{-2}
1G_4	3F_4	847.5	843.952	6.82×10^{-3}	8.12×10^{-3}		1.14×10^{-2}
1G_4	1G_4	943.8	918.056	8.47×10^{-2}	1.09×10^{-1}		6.70×10^{-2}
1H_5	1G_4	898.3	874.215	5.04×10^{-1}	3.98×10^{-1}	7.10×10^{-1}	6.54×10^{-1}
1P_1	3P_0	883.5	841.911	2.50×10^{-2}	2.64×10^{-2}		1.51×10^{-2}
1P_1	1S_0	982.2	972.174	5.21×10^{-1}	5.72×10^{-1}	9.20×10^{-1}	6.92×10^{-1}
1P_1	3P_1	883.8	843.782	5.41×10^{-6}	2.13×10^{-5}		
1P_1	3F_2	821.4	788.389	3.35×10^{-5}	4.98×10^{-5}		
1P_1	1D_2	864.3	825.777	1.14×10^{-2}	1.25×10^{-2}	2.00×10^{-2}	1.70×10^{-2}
1P_1	3P_2	887.5	847.449	3.43×10^{-3}	3.82×10^{-3}		2.83×10^{-3}
3D_1	3P_0	902.2	867.470	5.54×10^{-1}	5.55×10^{-1}	6.20×10^{-1}	7.76×10^{-1}
3D_1	1S_0	1043.8	1006.421	1.48×10^{-2}	1.59×10^{-2}		
3D_1	3P_1	902.5	869.458	6.03×10^{-2}	5.79×10^{-2}		7.64×10^{-2}
3D_1	3F_2	837.4	810.757	8.54×10^{-3}	1.09×10^{-2}	1.40×10^{-2}	2.19×10^{-2}
3D_1	1D_2	882.1	850.355	2.52×10^{-4}	2.95×10^{-4}		
3D_1	3P_2	906.6	873.353	3.40×10^{-5}	5.73×10^{-6}	6.00×10^{-3}	
3D_2	3P_1	904.7	868.976	3.97×10^{-1}	4.18×10^{-1}	4.60×10^{-1}	5.28×10^{-1}
3D_2	3F_2	839.2	810.340	2.84×10^{-4}	1.33×10^{-4}	2.60×10^{-3}	
3D_2	1D_2	884.1	849.855	1.01×10^{-2}	1.10×10^{-2}		9.14×10^{-3}
3D_2	3P_2	908.3	872.865	4.95×10^{-3}	4.48×10^{-3}		
3D_2	3F_3	819.2	814.840	1.24×10^{-2}	1.52×10^{-2}	1.40×10^{-2}	2.60×10^{-2}
3D_3	3F_2	835.8	806.673	4.10×10^{-3}	3.52×10^{-3}	7.00×10^{-5}	
3D_3	1D_2	880.3	845.864	1.31×10^{-1}	1.15×10^{-1}		1.32×10^{-1}
3D_3	3P_2	904.3	868.612	2.50×10^{-1}	2.45×10^{-1}		3.48×10^{-1}
3D_3	3F_3	814.3	811.137	1.22×10^{-3}	1.22×10^{-3}	1.70×10^{-3}	
3D_3	3F_4	818.8	816.461	6.19×10^{-3}	7.47×10^{-3}	1.60×10^{-2}	1.64×10^{-2}
3D_3	1G_4	908.4	885.621	1.96×10^{-3}	3.65×10^{-3}		1.22×10^{-2}
3F_2	3P_1	935.3	890.988	3.72×10^{-3}	4.07×10^{-3}		4.71×10^{-3}
3F_2	3F_2	856.9	829.448	1.45×10^{-1}	1.63×10^{-1}	1.50×10^{-1}	1.70×10^{-1}
3F_2	1D_2	903.8	870.939	6.53×10^{-3}	8.15×10^{-3}		1.32×10^{-2}
3F_2	3P_2	929.1	895.076	3.53×10^{-4}	3.77×10^{-4}		
3F_2	3F_3	836.1	834.159	1.00×10^{-2}	1.03×10^{-2}	1.30×10^{-2}	9.01×10^{-3}
3F_3	3F_2	855.7	827.855	6.14×10^{-2}	5.97×10^{-2}		1.15×10^{-1}
3F_3	1D_2	902.5	869.184	8.16×10^{-3}	7.37×10^{-3}		3.56×10^{-3}
3F_3	3P_2	927.7	893.226	7.76×10^{-3}	8.08×10^{-3}		9.80×10^{-3}
3F_3	3F_3	828.8	832.555	1.18×10^{-1}	1.26×10^{-1}	1.40×10^{-1}	1.13×10^{-1}
3F_3	3F_4	860.1	838.170	6.17×10^{-3}	6.63×10^{-3}		4.53×10^{-3}
3F_3	1G_4	934.2	911.214	6.46×10^{-5}	9.00×10^{-5}		4.74×10^{-4}
3F_4	3F_3	827.0	829.194	3.77×10^{-2}	3.68×10^{-2}		4.31×10^{-2}
3F_4	3F_4	831.8	834.768	1.29×10^{-1}	1.36×10^{-1}	1.60×10^{-1}	1.19×10^{-1}
3F_4	1G_4	931.8	907.198	1.29×10^{-2}	1.56×10^{-2}		2.12×10^{-2}

Table 3. *Continued.*

Initial	Final	λ	λ_{exp} [4]	f_{length}	f_{velocity}	f_{set} [6]	f_{set} [4]
3G_3	3F_2	845.7	819.534	4.03×10^{-1}	3.46×10^{-1}	5.80×10^{-1}	5.02×10^{-1}
3G_3	1D_2	891.3	860.015	3.06×10^{-2}	2.95×10^{-2}		1.48×10^{-2}
3G_3	3P_2	915.9	883.545	3.64×10^{-3}	4.17×10^{-3}		3.99×10^{-3}
3G_3	3F_3	820.3	819.534	5.45×10^{-2}	4.67×10^{-2}	5.80×10^{-1}	5.00×10^{-1}
3G_3	3F_4	822.4	829.640	5.78×10^{-4}	1.22×10^{-3}	4.60×10^{-4}	
3G_3	1G_4	923.4	901.149	4.24×10^{-4}	8.04×10^{-4}		3.20×10^{-3}
3G_4	3F_3	837.9	820.155	4.00×10^{-1}	3.40×10^{-1}	5.40×10^{-1}	4.84×10^{-1}
3G_4	3F_4	821.3	825.605	6.24×10^{-2}	5.40×10^{-2}		7.01×10^{-2}
3G_4	1G_4	918.3	896.387	4.75×10^{-4}	7.90×10^{-4}		
3G_5	3F_4	826.2	823.653	5.55×10^{-1}	4.08×10^{-1}	5.50×10^{-1}	5.70×10^{-1}
3H_4	3F_3	835.6	833.452	1.95×10^{-2}	1.72×10^{-2}		1.13×10^{-1}
3H_4	3F_4	840.4	839.078	3.02×10^{-3}	3.63×10^{-3}		6.25×10^{-3}
3H_4	1G_4	935.0	912.288	5.46×10^{-3}	6.75×10^{-3}		4.85×10^{-3}
3H_5	3F_4	841.3	836.570	8.33×10^{-3}	7.19×10^{-3}		1.89×10^{-2}
3H_5	1G_4	936.1	909.329	7.54×10^{-3}	5.52×10^{-3}		9.90×10^{-3}
3P_0	3P_1	867.4	858.310	6.26×10^{-2}	7.40×10^{-2}	9.90×10^{-2}	1.01×10^{-1}
3P_1	3P_0	889.4	857.461	7.67×10^{-2}	8.21×10^{-2}		8.13×10^{-2}
3P_1	1S_0	1026.8	992.970	7.12×10^{-3}	6.62×10^{-3}		
3P_1	3P_1	889.9	859.404	9.38×10^{-2}	9.95×10^{-2}		1.46×10^{-1}
3P_1	3F_2	826.4	802.008	9.70×10^{-4}	9.00×10^{-4}		
3P_1	1D_2	869.9	840.735	3.37×10^{-3}	3.68×10^{-3}		5.02×10^{-3}
3P_1	3P_2	893.8	863.206	5.22×10^{-2}	5.28×10^{-2}	7.50×10^{-2}	7.60×10^{-2}
3P_2	3P_1	895.3	861.022	2.60×10^{-3}	4.51×10^{-3}	1.20×10^{-1}	
3P_2	3F_2	831.2	803.419	3.97×10^{-5}	7.58×10^{-5}		
3P_2	1D_2	875.2	842.283	2.29×10^{-4}	2.19×10^{-4}		
3P_2	3P_2	898.9	864.837	2.18×10^{-1}	2.44×10^{-1}	2.30×10^{-1}	3.10×10^{-1}
3P_2	3F_3	811.5	807.846	1.54×10^{-3}	1.90×10^{-3}		

**Fig. 1.** Relative difference between the theoretical wavelengths calculated in this work and the experimental results by Reader and Acquista [4].

It is worthwhile to call attention to the strong mixing between the $4d4f$ 3D_3 and $4d4f$ 1F_3 levels predicted by these authors [4], which was confirmed by our calculations. We found the following LS percentage composition for each wave function:

- 1F_3 wave function \rightarrow 43% 1F_3 and 44% 3D_3 ;
- 3D_3 wave function \rightarrow 45% 1F_3 and 53% 3D_3 .

For all the other $4d4f$ levels, the percentage of the LSJ wave functions shown on the Table 3 is greater than 80%.

A general agreement between length and velocity forms of the oscillator strengths is found; in 79% of our results the length and velocity forms of the oscillator strengths differ by less than 20% and in 54% of our results the two forms differ by less than 10%. The transition shown in Table 1 is a case where a significant discrepancy remains between the two forms of the oscillator strength, after inclusion of correlation. On the other hand, Table 2 illustrates an example where good agreement between length and velocity forms is achieved after inclusion of correlation.

4 Conclusions

We presented *ab initio* relativistic calculated values of wavelengths and oscillator strengths for all $4d4f \rightarrow 4d^2$ dipole-allowed transitions in Zr III. These transitions are of interest because of their importance in the interpretation of spectra from some chemically peculiar stars. We show that inclusion of correlation is important. The results are compared with existing semi-empirical theoretical calculations and with experimental data.

This research was supported in part by FCT project POCTI/FAT/44279/2002 financed by the European Community Fund FEDER. The authors thank Doctors Jean-Paul Desclaux and Paul Indelicato for advice in the use of their MCDF code.

References

1. *Upper main sequence stars with anomalous abundances, 90th Colloq. IAU* edited by C.R. Cowley, M.M. Dworetzky (D. Reidel, Dordrecht, 1986)
2. A. Redfors, *Astron. Astrophys.* **249**, 589 (1991)
3. D.S. Leckrone, S. Johansson, G.M. Wahlgren, S. Adelman, *Phys. Scr.* **47**, 149 (1993)
4. J. Reader, N. Acquista, *Phys. Scr.* **55**, 310 (1997)
5. Z.A. Khan, M.S.Z. Chaghtai, K. Rahimullah, *Phys. Scr.* **23**, 29 (1981)
6. E. Charro, J.L. López-Ayuso, I. Martín, *J. Phys. B* **32**, 4555 (1999)
7. J.P. Desclaux, *Comp. Phys. Commun.* **9**, 31 (1975)
8. P. Indelicato, *Phys. Rev. Lett.* **77**, 3323 (1996)
9. P. Indelicato, *Phys. Rev. A* **51**, 1132 (1995)
10. G.E. Brown, D.E. Ravenhall, *Proc. R. Soc. Lond. A* **208**, 552 (1951)
11. J. Sucher, *Phys. Rev. A* **22**, 348 (1980)
12. M.H. Mittleman, *Phys. Rev. A* **24**, 1167 (1981)
13. O. Gorceix, P. Indelicato, *Phys. Rev. A* **37**, 1087 (1988)
14. E. Lindroth, A.-M. Mårtensson-Pendrill, *Phys. Rev. A* **39**, 3794 (1989)
15. P.J. Mohr, *Phys. Rev. A* **26**, 2338 (1982)
16. P.J. Mohr, Y.-K. Kim, *Phys. Rev. A* **45**, 2727 (1992)
17. P.J. Mohr, *Phys. Rev. A* **46**, 4421 (1992)
18. P. Indelicato, O. Gorceix, J.P. Desclaux, *J. Phys. B* **20**, 651 (1987)
19. P. Indelicato, J.P. Desclaux, *Phys. Rev. A* **42**, 5139 (1990)
20. P. Indelicato, P.J. Mohr, *Phys. Rev. A* **63**, 4052507 (2001)
21. S.A. Blundell, *Phys. Rev. A* **46**, 3762 (1992)
22. S.A. Blundell, *Phys. Scr.* **T46**, 144 (1993)
23. P. Indelicato, *Hyp. Int.* **108**, 39 (1997)
24. P.-O. Löwdin, *Phys. Rev.* **97**, 1474 (1955)
25. A. Hibbert, *Phys. Scr.* **65**, 104 (1996)
26. A. Hibbert, *J. Phys. B* **36**, 4703 (2003)
27. A.F. Starace, *Phys. Rev. A* **3**, 1242 (1971)
28. A.F. Starace, *Phys. Rev. A* **8**, 1141 (1971)
29. A. Derevianko, I.M. Savukov, W.R. Johnson, D.R. Plante, *Phys. Rev. A* **58**, 4453 (1998)